Ionics (2012) 18:249–254
DOI 10.1007/s11581-011-0628-1

ORIGINAL PAPER

Effect of LiBOB as additive on electrochemical properties of lithium–sulfur batteries

Shizhao Xiong · Xie Kai · Xiaobin Hong · Yan Diao

Received: 22 June 2011 / Revised: 9 September 2011 / Accepted: 9 September 2011 / Published online: 27 September 2011

Abstract The effect of varying amounts (in the range 1–10 wt.%) of LiBOB (lithium bis(oxalato) borate) as additive in mixed liquid electrolyte on the electrochemical performance of lithium–sulfur batteries is investigated at room temperature. The electrochemical impedance spectroscopy (EIS) of lithium anode with LiBOB has two semicircles, corresponding to charge transfer impedance and ion migration impedance, respectively. The lithium anode with LiBOB shows a higher ion migration impedance, which could reduce the ionic diffusion rate in the anode. Scanning electron microscopy (SEM) observations shows that lithium anode with LiBOB has a smoother and denser surface morphology than the anode without LiBOB. The lithium–sulfur batteries with LiBOB shows the improvement of both the discharge capacity and cycle performance, a maximum discharge capacity of 1,191 mA h g^{-1} is obtained with 4 wt.% LiBOB. The lithium–sulfur batteries with 4 wt.% LiBOB can maintain a reversible capacity of 756 mA h g^{-1} after 50 cycles.

Keywords Lithium–sulfur batteries · Lithium bis(oxalato) borate · Additive · Lithium anode

Introduction

Batteries are currently being developed to power an increasingly diverse range of applications, from cars to microchips. All along, researchers have been their best to build better batteries for modern-day demands [1]. High energy density is one of the hottest topics in the field of lithium-ion batteries, which is why lithium–sulfur batteries have been extensively studied during the past few decades. The theoretical energy density of the lithium–sulfur batteries is about 2,600 Wh kg^{-1}, more than five times the theoretical energy of commercial lithium-ion batteries [2]. At the same time, the lithium–sulfur batteries are made of inexpensive and nontoxic materials. Hence, there is a strong incentive to develop rechargeable lithium–sulfur batteries [3–5].

Despite its considerable advantages, the lithium–sulfur battery is plagued with problems that have hindered its widespread application [5, 6]. Capacity degradation on repeated discharge–charge of batteries is one of the major hurdles [7]. This is mainly due to the high solubility of the polysulfides formed as reaction intermediates in both discharge and charge processes in the polar organic solvents used in electrolytes [8]. During cycling, the polysulphide anions can migrate through the separator to the lithium anode, whereupon they are reduced to solid precipitates (Li_2S_2 and/or Li_2S), causing active mass loss [5, 9]. In response to these considerable challenges, novel advances in materials design such as new electrolytes [10–13], new sulfur cathode [14–16] and protective films for the lithium anode [9, 17] have been developed to overcome these challenges. Meanwhile, achievements of electrolyte modification and cathode preparation have resulted in some promising results [18, 19], but much of the difficulty remains at the protection of lithium anode. The methods of protecting lithium anode at present are too costly and complex to generalize the practical application of lithium–sulfur batteries.

Additive in electrolyte is a major usual method to modify the electrode/electrolyte interface in lithium-ion batteries [20]. $LiNO_3$ has been investigated as an additive in electrolyte for

S. Xiong (✉) · X. Kai · X. Hong · Y. Diao
Department of Material Engineering and Applied Chemistry, School of Aerospace and Material Engineering, National University of Defense Technology, Changsha, Hunan 410073, China
e-mail: sxiong@nudt.edu.cn

lithium–sulfur batteries by Aurbach and co-workers [21]. It was shown that solvents, polysulfide and $LiNO_3$ additives reacted with lithium to form protective surface film on lithium anode; the film prevented parasitic reaction between lithium anode and polysulfides, which contributed to active mass loss. Hence, the cycle life and discharge capacity of lithium–sulfur batteries was improved. But it is hard for the surface film to maintain stability with the increased surface roughness of lithium anode during cycling, because the film with inorganic species is devoid of tenacity. Another issue is the reduced safety of lithium–sulfur batteries. Because the component of sulfur cathodes such as carbon and sulfur [5] has a strong deoxidization, the presence of $LiNO_3$ with strong oxidation increases the potential risks of the batteries.

For this reason, it is necessary to explore a new additive in electrolyte for lithium–sulfur batteries. LiBOB is a potential candidate salt for use in lithium ion batteries [22, 23]. It has several advantages: it is thermally more stable; it more environment-friendly because its hydrolytic decomposition products are less toxic and corrosive; and it actively takes part in the formation of a stable solid electrolyte interface film on the graphite negative electrode [24, 25]. The solid electrolyte interface film formed with LiBOB improves the electrochemical properties of graphite electrode due to its tenacity and denseness [24, 26].

In the present work, we investigated the effect of LiBOB as additive on the electrochemical properties of lithium–sulfur batteries, with an aim to modify the interface between electrolyte and lithium anode. Finally, the modified interface enhanced the electrochemical performance of lithium–sulfur batteries by preventing the parasitic reaction between lithium anode and polysulfides in electrolyte, which causes active mass loss.

Experimental

Preparation of electrolyte and lithium–sulfur cell

The pure electrolytes consisted of either 1 M $LiN(CF_3SO_2)_2$ in DIOX and DME (1:1, v/v, Novolyte) mixed solvents. LiBOB (Novolyte) was also used as additive to the $LiN(CF_3SO_2)_2$ electrolyte by weight.

Active cathode material sulfur (99.98%, Aldrich) and the conducting agent acetylene black (Alfa) were dried at 50°C and 120°C, respectively, under vacuum for 24 h before use. The specific surface of acetylene black is 910 $m^2\ g^{-1}$. To prepare the sulfur cathode, 60 wt.% of sulfur, 25 wt.% of acetylene black and 15 wt.% of poly(vinylidene fluoride-*co*-hexafluoropropene) binder were taken in NMP solvent and mixed in a Spex ball mill at room temperature for 2 h at 580 rev/min. The slurry was coated on an aluminum current collector, dried for 24 h at room temperature and further at 60°C under vacuum for 12 h. The sulfur cathode film so obtained was uniformly pressed to 50-μm thickness using a roll press, and the specific surface of sulfur cathode prepared is 54 $m^2\ g^{-1}$.

The sulfur cathode, lithium anode (100 μm; Denway, China) and a porous polyolefin separator (Celgard® 2500) were combined into a layered structure of cathode/separator/anode that was wound and compressed, with an electrode area of about 210 cm^2 and an electrolyte mass of about 3.2 g. The specific capacity is based on the mass of element sulfur. The assembled cell was sealed with an appropriate amount of the electrolyte in an aluminum- plastic pack under vacuum.

Characterization

The morphological features of the lithium anodes were observed using scanning electron microscope (SEM) (HTACHI S-4800). The charge–discharge and cycling tests were performed between 1.7 and 2.4 V at room temperature using on a multi-channel batteries tester (LAND CT2001A) operating in galvanostatic mode. Impedance of lithium anode was measured using AUTOLAB (AUT71864) over a frequency range of 100 mHz to 1 MHz. The lithium anode was pulled out of the cell after the first cycle, and then washed by the electrolyte used in cell. After that, the lithium anode was cut into oblong shapes (3×4 mm) to assemble the system for impedance measurement. A conventional two-electrode system was used for the impedance measurements, using two lithium anodes with the same area as electrodes.

Results and discussion

Impedance analyzing of lithium anode

Figure 1 shows the AC impedance of lithium anode with different contents of LiBOB in the electrolyte. Each impedance spectrum was measured while the electrode was in equilibrium. A major variation of impedance spectrum was observed with LiBOB addition; the lithium anode with LiBOB displayed two semicircles while lithium anode without LiBOB displayed only one. As already discussed in detail [27, 28], the two semicircles in the impedance spectra has been interpreted as resulting from two kinds of passivating films. The high-frequency semicircle relates to the first passivating surface film, and the low-frequency semicircle relates to the second. The change in resistance for the first film has been found to increase with an increase of lithium salt concentration. As shown in Fig. 1, the lithium anode with LiBOB had two kinds of passivating films, while lithium anode without LiBOB only had one. It can be suggested that the second semicircle of

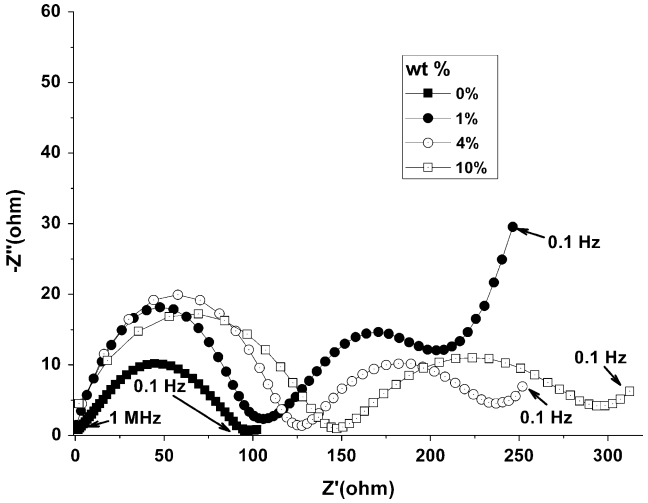

Fig. 1 AC impedance of lithium anode with different concentration of LiBOB in the electrolyte. The data were collected after the first cycle

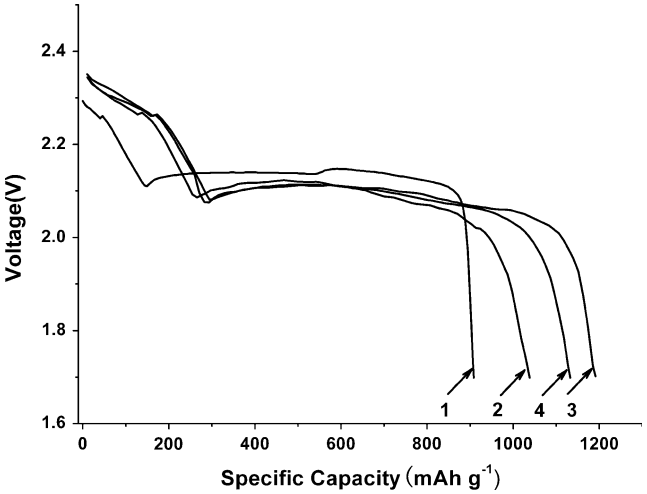

Fig. 2 Discharge curves of lithium–sulfur batteries with varying content (wt.%) of LiBOB as additive: *1* wt.0%, *2* 1 wt.%, *3* 4 wt.%, *4* 10 wt.%

lithium anode without LiBOB was so small that the two semicircles could not be separated. Furthermore, the first passivating surface film resistance of lithium anode with LiBOB increased with an increase in LiBOB concentration. It can be suggested that the thickness of the first passivating surface film formed on lithium anode with LiBOB increases with the increasing content of LiBOB. At the same time, the second passivating surface film formed on lithium anode with LiBOB is probably more closely related to the effect of LiBOB on electrochemical properties of lithium–sulfur batteries.

Electrochemical performance of lithium–sulfur batteries

Figure 2 shows the discharge curves of lithium–sulfur batteries with varying contents of LiBOB as additive. The discharge process of lithium–sulfur batteries can be divided in the first discharge plateau (high plateau, 2.4–2.1 V), where the reduction of elemental sulfur to form soluble polysulfides and further reduction of the soluble polysulfide occur, and the second discharge plateau (low plateau, 2.1–1.5 V), where the soluble polysulfides are reduced to form Li_2S solid film [29]. As shown in Fig. 2, the overall discharge profile of lithium–sulfur batteries with LiBOB was quite similar to that without LiBOB. Both of them had high plateau and low plateau, but the high plateau of lithium–sulfur batteries with LiBOB was obviously longer than that without LiBOB. This can be reasonably attributed to the shuttle phenomenon in lithium–sulfur batteries. The higher-order polysulfides, which are generated at the sulfur cathode during the first discharge plateau, diffuse to the lithium anode where they react directly with the lithium anode in a parasitic reaction to recreate the lower-order polysulfides [30]. This resulted in the loss of active mass in the first discharge plateau and the reduction of voltage. This result suggests that LiBOB as additive can prevent the parasitic reaction between higher polysulfides and lithium anode.

The variations of the capacities of different plateaus with varying contents of LiBOB are shown in Fig. 3. The capacity of high plateau increased with adding LiBOB, but was maintained at 300 mA h g^{-1} with the increasing content of LiBOB. This suggests that the passivating surface film formed with 4 wt.% LiBOB is enough to prevent the parasitic reaction. However, the capacity of low plateau with varying contents of LiBOB showed a different trend: it increased with the content of LiBOB under 4 wt.%, and then depressed with the content of LiBOB over 4 wt.% It can be attributed to the increasing Li-ion migration

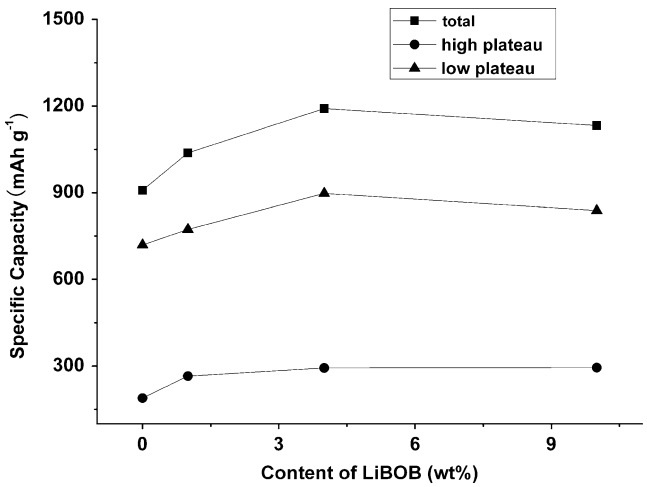

Fig. 3 Variations in the capacities of different plateaus with varying contents of LiBOB

impedance. During the high plateau, formation of soluble polysulfide increases the viscosity of the electrolyte medium, resulting in the low lithium-ion diffusion in electrolyte [31]. As a consequence, the significant polarization will occur at the low plateau, which can be exhibited by the depressed discharge voltage. As shown in Fig. 2, the discharge voltage of low plateau decreased with the addition of LiBOB. This result suggests that the increasing content of LiBOB over 4 wt.% leads to the increase in Li-ion migration impedance, resulting in depressed capacity of low plateau.

Figure 4 shows charge curves of lithium–sulfur batteries with varying contents of LiBOB as additive. The charge process of the lithium–sulfur batteries could also be divided into the first charge plateau (low plateau, 2.2–2.33 V) where the oxidation of solid Li_2S to form soluble polysulfides and further oxidation of the soluble polysulfide occur, and the second charge plateau (high plateau, 2.33–2.4 V) where the soluble polysulfides are oxidated to higher-order polysulfides and the higher-order polysulfides are oxidated to element sulfur. As discussed in previous sections, the higher-order polysulfides diffuse to the lithium electrode where they react directly with the lithium anode in a parasitic reaction to recreate the lower-order polysulfides. These species diffuse back to the sulfur electrode to generate the higher-order polysulfide again, thus creating a shuttle mechanism [30]. As shown in Fig. 4, the lithium–sulfur batteries without LiBOB never reached complete charge and showed a voltage leveling. It indicates that the charge current is lower than the shuttle current, which means that the parasitic reaction between higher polysulfides and lithium anode is very active. The charge curves of lithium–sulfur batteries showed an obvious change after adding LiBOB. With the increasing content of LiBOB, the charge curve showed a sharper voltage increase. With the same charge current, this indicates that the shuttle current depressed with the addition of LiBOB. The results shown in Figs. 2 and 4 strongly suggest that the parasitic reaction between higher polysulfides and lithium anode is prevented after adding LiBOB in the electrolyte. In addition, with the increasing content of LiBOB, the preventative effect becomes more obvious.

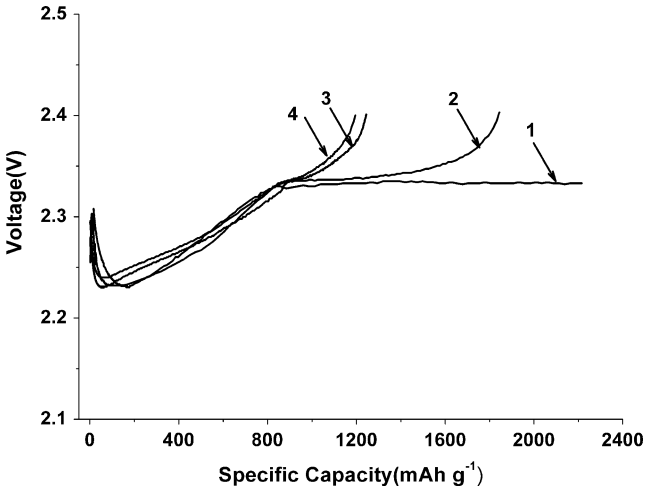

Fig. 4 Charge curves of lithium–sulfur batteries with varying contents (wt.%) of LiBOB as additive: *1* 0 wt.%, *2* 1 wt.%, *3* 4 wt.%, *4* 10 wt.%; current density: 0.24 m A cm^{-2}

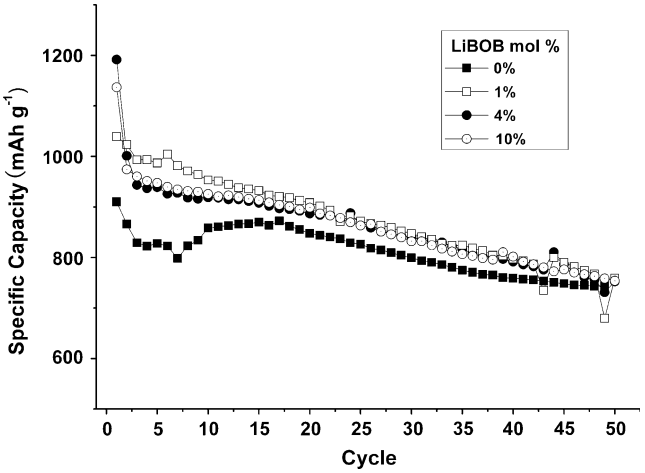

Fig. 5 Cycle performance of lithium–sulfur batteries with varying contents of LiBOB

Figure 5 shows the cycle performance of lithium–sulfur batteries with varying contents of LiBOB. The poor cycle performance of lithium–sulfur batteries was mainly attributed to the formation of irreversible Li_2S [31], structure invalidation of cathode's matrix [6, 7] and the parasitic reaction between higher polysulfides and lithium anode [9, 30]. As shown in Fig. 5, the cycle performance of lithium–sulfur batteries with LiBOB was significantly improved in the first 20 cycles. It can be preferably explained that the parasitic reaction between higher polysulfides and lithium anode is the main factor leading to the capacity fading in early cycles. However, the impact of adding LiBOB became unobvious with the increasing cycles. It suggests that the capacity fading of lithium–sulfur batteries in evening cycles can be mainly attributed to other factors. Different from the capacity variety with contents of LiBOB, the lithium–sulfur batteries with 1 wt.% LiBOB showed better cycle performance. This result can be attributed to the increasing Li-ion migration impedance. This suggests that the passivating surface film formed with 1 wt.% LiBOB is enough to prevent the parasitic reaction after cycling.

Surface morphology of lithium anode

Figure 6 compares the surface morphology of lithium anode with and without LiBOB after 50 cycles. The

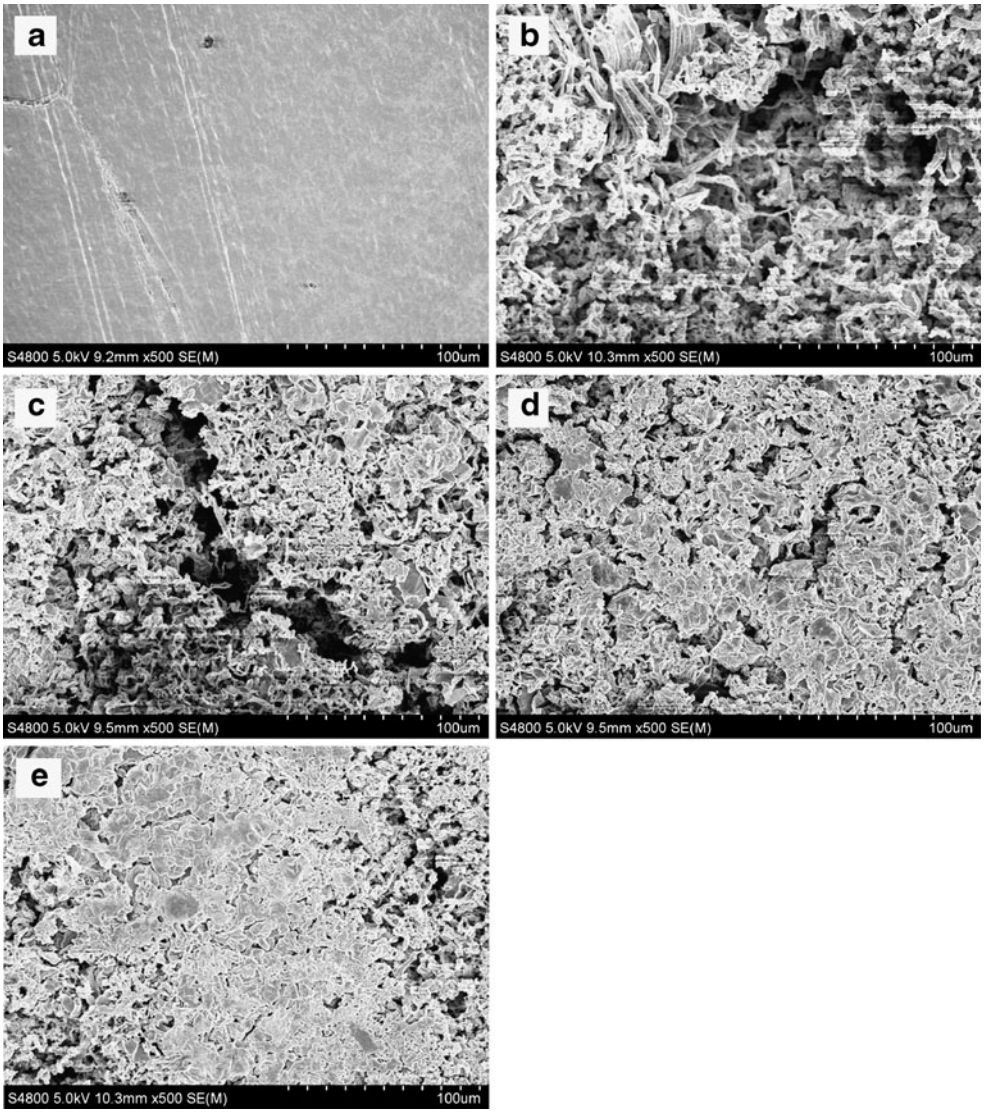

Fig. 6 Surface morphologies of lithium anode after 50 cycles: **a** before cycling, **b** without additive; **c** with 1 wt.% LiBOB, **d** with 4 wt.% LiBOB, **e** with 10 wt.% LiBOB

surface of lithium anode before cycling was smooth, compact and almost featureless, except for a few holes and ravines. However, considering the needlelike dendrites growing to the surface of the lithium anode after cycling, the species of dendrites could be products produced by the reaction between species of electrolyte and lithium anode [32]. The needlelike dendrites cause two problems: the failure of lithium anode structure and the increasing possibility of short circuit in batteries. Furthermore, the problems result in poor cycle life and safety of batteries, respectively. As shown in Fig. 6, with the addition of LiBOB, the lithium anode after cycling showed a smoother and denser surface morphology. The roughness of the surface morphology reduced with the increasing content of LiBOB. As discussed in previous sections, this result demonstrates that LiBOB as additive can prevent the reaction between species of electrolyte and lithium anode.

Conclusions

The effect of LiBOB as additive on the electrochemical properties of lithium–sulfur batteries was investigated. The batteries with LiBOB showed higher discharge capacity, lower charge capacity and better cycle performance, which seemed to be due to the formation of passivating surface film on lithium anode. The passivating surface film could prevent the parasitic reaction between higher polysulfides and lithium anode, which resulted in the shuttle phenomenon in lithium–sulfur batteries. At the same time, it increased the Li-ion migration impedance and charge transfer impedance of lithium anode. Thus, the appropriate content was as important as the adding of LiBOB. The surface morphologies of lithium anode after cycling showed that the lithium anode with LiBOB had a smoother and denser surface morphology. For further understanding of this phenomenon, the species of passivating surface film

formed on lithium anode should be taken into theoretical and experimental consideration.

References

1. Armand M, Tarascon JM (2008) Nature 451:652
2. Yamin H, Gorenshtein A, Penciner J, Sternberg Y, Peled E (1988) J Electrochem Soc 135:1045
3. Kolosnitsyn VS, Karaseva EV, Seung DY, Cho MD (2003) Russ J Electrochem 39:1218
4. He X, Ren J, Wang L, Pu W, Wan C, Jiang C (2009) Ionics 15:477
5. Ji X, Lee KT, Nazar LF (2009) Nat Mater 2460:500
6. Elazari R, Salitra G, Talyosef Y, Grinblat J, Kelley CS, Xiao A, Affinito J, Aurbach D (2010) J Electrochem Soc 157:A1131
7. Cheon SE, Choi SS, Han JS, Choi YS, Jung BH, Lima HS (2004) J Electrochem Soc 151:A2067
8. Choi JW, Kim JK, Cheruvally G, Ahna JH, Ahnb HJ, Kimb KW (2007) Electrochim Acta 52:2075
9. Lee YM, Choi NS, Park JH, Park JK (2003) J Power Sources 119:964
10. Shin JH, Cairns EJ (2008) J Electrochem Soc 155:A368
11. Wang Y, Huang Y, Huang C, Wang W, Yu Z, Zhang H, Wang A, Yuan K (2009) J Appl Electrochem 40:321
12. Yuan LX, Feng JK, Ai XP, Cao YL, Chen SL, Yang HX (2006) Electrochem Commun 8:610
13. Wang J, Chew SY, Zhao ZW, Ashraf S, Wexler D, Chen J, Ng SH, Chou SL, Liu HK (2008) Carbon 46:229
14. Liang C, Dudney NJ, Howe JY (2009) Chem Mater 21:4724
15. Pu W, He X, Wang L, Tian X, Jiang C, Wan C (2007) Ionics 13:273
16. Wang L, He X, Ren J, Pu W, Li J, Gao J (2010) Ionics 16:689
17. Mikhaylik YV (2005) US Pat 0,147,891
18. Mikhaylik YV (2008) US Pat 7,354,680
19. Akridge JR, Mikhaylik YV, White N (2004) Solid State Ionics 175:243
20. Aurbach D, Gamolsky K, Markovsky B, Gofer Y, Schmidt M, Heider U (2002) Electrochim Acta 47:1423
21. Aurbach D, Pollak E, Elazari R, Salitra G, Kelley CS, Affinitob J (2009) J Electrochem Soc 156:A694
22. Xu K, Zhang SS, Lee U, Allen JL, Jow TR (2005) J Power Sources 146:79
23. Xu K, Zhang S, Jow R (2005) J Power Sources 143:197
24. Täubert C, Fleischhammer M, Wohlfahrt-Mehrens M, Wietelmann U, Buhrmesterb T (2010) J Electrochem Soc 157:A721
25. Kaneko H, Sekine K, Takamura T (2005) J Power Sources 146:142
26. Xu K, Zhang S, Jow TR (2003) Electrochem Solid-State Lett 6: A117
27. Takami N, Ohsaki T, Inada K (1992) J Electrochem Soc 139:1849
28. Chen Z, Lu WQ, Liu K, Amine K (2006) Electrochim Acta 51:3322
29. Cheon SE, Ko KS, Cho JH, Kim SW, Chin EY (2003) J Electrochem Soc 150:A796
30. Mikhaylik YV, Akridge JR (2004) J Electrochem Soc 151:A1969
31. Cheon SE, Ko KS, Cho JH, Kim SW, Chin EY (2003) J Electrochem Soc 150:A800
32. López CM, Vaughey JT, Dees DE (2009) J Electrochem Soc 156: A726